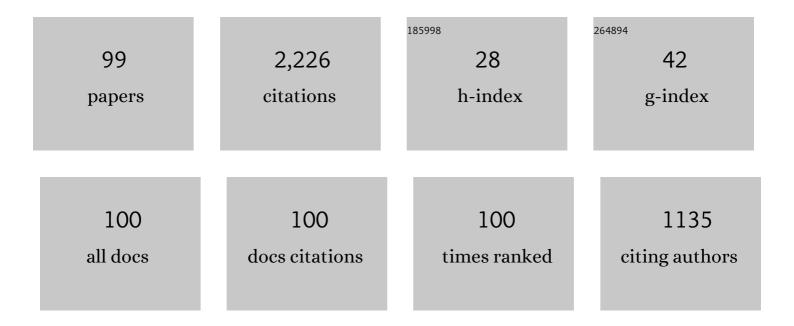
List of Publications by Year in descending order

Source: https://exaly.com/author-pdf/2895785/publications.pdf Version: 2024-02-01



#	Article	IF	CITATIONS
1	Climatic and tectonic controls of lacustrine hyperpycnite origination in the Late Triassic Ordos Basin, central China: Implications for unconventional petroleum development. AAPG Bulletin, 2017, 101, 95-117.	0.7	143
2	Lithofacies and origin of the Late Triassic muddy gravity-flow deposits in the Ordos Basin, central China. Marine and Petroleum Geology, 2017, 85, 194-219.	1.5	96
3	An extensive erosion surface of a strongly deformed limestone bed in the Gushan and Chaomidian formations (late Middle Cambrian to Furongian), Shandong Province, China: Sequence–stratigraphic implications. Sedimentary Geology, 2011, 233, 129-149.	1.0	88
4	Calcite precipitation induced by Bacillus cereus MRR2 cultured at different Ca2+ concentrations: Further insights into biotic and abiotic calcite. Chemical Geology, 2018, 500, 64-87.	1.4	87
5	Cambrian stratigraphy of the North China Platform: revisiting principal sections in Shandong Province, China. Geosciences Journal, 2010, 14, 235-268.	0.6	78
6	Limestone pseudoconglomerates in the Late Cambrian Gushan and Chaomidian Formations (Shandong) Tj ETQqQ	0 0 rgBT 1.6	/Overlock 10 68
7	FURONGIAN (LATE CAMBRIAN) SPONGE-MICROBIAL MAZE-LIKE REEFS IN THE NORTH CHINA PLATFORM. Palaios, 2014, 29, 27-37.	0.6	67
8	Classification of gravity-flow deposits and their significance for unconventional petroleum exploration, with a case study from the Triassic Yanchang Formation (southern Ordos Basin, China). Journal of Asian Earth Sciences, 2018, 161, 57-73.	1.0	52
9	Mechanism of Biomineralization Induced by Bacillus subtilis J2 and Characteristics of the Biominerals. Minerals (Basel, Switzerland), 2019, 9, 218.	0.8	52
10	Geochronology and geochemistry of Permo-Triassic sandstones in eastern Jilin Province (NE China): Implications for final closure of the Paleo-Asian Ocean. Geoscience Frontiers, 2019, 10, 683-704.	4.3	51
11	Cementation and porosity evolution of tight sandstone reservoirs in the Permian Sulige gas field, Ordos Basin (central China). Marine and Petroleum Geology, 2019, 103, 276-293.	1.5	49
12	A stem-group cnidarian described from the mid-Cambrian of China and its significance for cnidarian evolution. Nature Communications, 2011, 2, 442.	5.8	47
13	Depositional and Diagenetic Controls on Sandstone Reservoirs with Low Porosity and Low Permeability in the Eastern Sulige Gas Field, China. Acta Geologica Sinica, 2014, 88, 1513-1534.	0.8	47
14	Funnel-shaped, breccia-filled clastic dykes in the Late Cambrian Chaomidian Formation (Shandong) Tj ETQq0 0 0 r	gBT/Over	rlock 10 Tf 50
15	Sequence-stratigraphic comparison of the upper Cambrian Series 3 to Furongian succession between the Shandong region, China and the Taebaek area, Korea: high variability of bounding surfaces in an epeiric platform. Geosciences Journal, 2012, 16, 357-379.	0.6	46

16	Early diagenetic deformation structures of the Furongian ribbon rocks in Shandong Province of China—A new perspective of the genesis of limestone conglomerates. Science China Earth Sciences, 2010, 53, 241-252.	2.3	43
17	Diagenesis and porosity evolution of sandstone reservoirs in the East II part of Sulige gas field, Ordos Basin. International Journal of Mining Science and Technology, 2012, 22, 311-316.	4.6	43
	Source analysis of quartz from the Upper Ordovician and Lower Silurian black shale and its effects		

¹⁸on shale gas reservoir in the southern Sichuan Basin and its periphery, China. Geological Journal,0.6432019, 54, 438-449.

#	Article	IF	CITATIONS
19	Geochemistry and geochronology of Upper Permian–Upper Triassic volcanic rocks in eastern Jilin Province, NE China: implications for the tectonic evolution of the Palaeo-Asian Ocean. International Geology Review, 2017, 59, 368-390.	1.1	42
20	The bio-precipitation of calcium and magnesium ions by free and immobilized Lysinibacillus fusiformis DB1-3 in the wastewater. Journal of Cleaner Production, 2020, 252, 119826.	4.6	40
21	C5–C13 light hydrocarbons of crude oils from northern Halahatang oilfield (Tarim Basin, NW China) characterized by comprehensive two-dimensional gas chromatography. Journal of Petroleum Science and Engineering, 2017, 157, 223-231.	2.1	38
22	Late Mesozoic and Cenozoic tectono-thermal history and geodynamic implications of the Great Xing'an Range, NE China. Journal of Asian Earth Sciences, 2020, 189, 104155.	1.0	37
23	Bio-precipitation of Calcite with Preferential Orientation Induced by <i>Synechocystis</i> sp. PCC6803. Geomicrobiology Journal, 2014, 31, 884-899.	1.0	34
24	Calcium carbonate precipitation by Synechocystis sp. PCC6803 at different Mg/Ca molar ratios under the laboratory condition. Carbonates and Evaporites, 2017, 32, 561-575.	0.4	34
25	From divergent to convergent plates: Resulting facies shifts along the southern and western margins of the Sino-Korean Plate during the Ordovician. Journal of Geodynamics, 2019, 129, 149-161.	0.7	32
26	A Marine or Continental Nature of the Deltas in the Early Cretaceous Lingshandao Formation-Evidences from Trace Elements. Acta Geologica Sinica, 2017, 91, 367-368.	0.8	31
27	The Significant Roles of Mg/Ca Ratio, Clâ^' and SO42â^' in Carbonate Mineral Precipitation by the Halophile Staphylococcus epidermis Y2. Minerals (Basel, Switzerland), 2018, 8, 594.	0.8	31
28	Origin of the vertically orientated clasts in brecciated shallowâ€marine limestones of the Chaomidian Formation (Furongian, Shandong Province, China). Sedimentology, 2013, 60, 1059-1070.	1.6	29
29	The Characterization of Intracellular and Extracellular Biomineralization Induced by <i>Synechocystis sp</i> . PCC6803 Cultured under Low Mg/Ca Ratios Conditions. Geomicrobiology Journal, 2017, 34, 362-373.	1.0	27
30	Struvite Precipitation Induced by a Novel Sulfate-Reducing BacteriumAcinetobacter calcoaceticusSRB4 Isolated from River Sediment. Geomicrobiology Journal, 2015, 32, 868-877.	1.0	26
31	Precipitation of Carbonate Minerals Induced by the Halophilic Chromohalobacter Israelensis under High Salt Concentrations: Implications for Natural Environments. Minerals (Basel, Switzerland), 2017, 7, 95.	0.8	26
32	Extracellular and Intracellular Biomineralization Induced by Bacillus licheniformis DB1-9 at Different Mg/Ca Molar Ratios. Minerals (Basel, Switzerland), 2018, 8, 585.	0.8	26
33	The influence of hyperpycnal flows on the salinity of deep-marine environments, and implications for the interpretation of marine facies. Marine and Petroleum Geology, 2018, 98, 1-11.	1.5	26
34	Biomineralization of Monohydrocalcite Induced by the Halophile Halomonas smyrnensis WMSâ€3. Minerals (Basel, Switzerland), 2019, 9, 632.	0.8	26
35	Cambrian oncoids and other microbial-related grains on the North China Platform. Carbonates and Evaporites, 2015, 30, 373-386.	0.4	25
36	Zircon U–Pb geochronology and geochemistry of the post-collisional volcanic rocks in eastern Xinjiang Province, NW China: implications for the tectonic evolution of the Junggar terrane. International Geology Review, 2018, 60, 339-364.	1.1	25

#	Article	IF	CITATIONS
37	Construction of Time-Space Structure Model of Deep Stope and Stability Analysis. Polish Journal of Environmental Studies, 2016, 25, 2633-2639.	0.6	25
38	Basin modeling in the initial stage of exploration: a case study from the North Subbasin of the South Yellow Sea Basin. Acta Oceanologica Sinica, 2017, 36, 65-78.	0.4	23
39	Bio-Precipitation of Calcium and Magnesium Ions through Extracellular and Intracellular Process Induced by Bacillus Licheniformis SRB2. Minerals (Basel, Switzerland), 2019, 9, 526.	0.8	22
40	Hydrocarbon Generation Evaluation, Burial History, and Thermal Maturity of the Lower Triassic–Silurian Organic-Rich Sedimentary Rocks in the Central Uplift of the South Yellow Sea Basin, East Asia. Energy & Fuels, 2020, 34, 4565-4578.	2.5	22
41	Precipitation of calcite induced by Synechocystis sp. PCC6803. World Journal of Microbiology and Biotechnology, 2013, 29, 1801-1811.	1.7	21
42	Thermogravimetric and kinetic analysis of thermal decomposition characteristics of microbial calcites induced by cyanobacteria Synechocystis sp. PCC6803. Journal of Thermal Analysis and Calorimetry, 2017, 127, 1371-1379.	2.0	21
43	Constraints of zircon U-Pb-Hf isotopes from Late Permian-Middle Triassic flora-bearing strata in the Yanbian area (NE China) on a scissor-like closure model of the Paleo-Asian Ocean. Journal of Asian Earth Sciences, 2019, 183, 103964.	1.0	21
44	Characterization of calcium deposition induced by Synechocystis sp. PCC6803 in BG11 culture medium. Chinese Journal of Oceanology and Limnology, 2014, 32, 503-510.	0.7	20
45	Recovery of phosphate, magnesium and ammonium from eutrophic water by struvite biomineralization through free and immobilized Bacillus cereus MRR2. Journal of Cleaner Production, 2021, 320, 128796.	4.6	20
46	Characteristics and genesis of microbial lumps in the Maozhuang Stage (Cambrian Series 2), Shandong Province, China. Science China Earth Sciences, 2013, 56, 494-503.	2.3	19
47	Isolation of <i>Leclercia adcarboxglata</i> Strain JLS1 from Dolostone Sample and Characterization of its Induced Struvite Minerals. Geomicrobiology Journal, 2017, 34, 500-510.	1.0	18
48	Early-Middle Ordovician intermediate-mafic and ultramafic rocks in central Jilin Province, NE China: geochronology, origin, and tectonic implications. Mineralogy and Petrology, 2019, 113, 393-415.	0.4	16
49	Two middle Cambrian trilobite genera, <i>Cyclolorenzella</i> Kobayashi, 1960 and <i>Jiulongshania</i> gen. nov., from Korea and China. Alcheringa, 2008, 32, 247-269.	0.5	15
50	New Evidence of Detrital Zircon Ages for the Final Closure Time of the Paleo-Asian Ocean in the Eastern Central Asian Orogenic Belt (NE China). Acta Geologica Sinica, 2017, 91, 1910-1914.	0.8	15
51	Ontogeny of the Middle Cambrian Trilobite Shantungia spinifera Walcott, 1905 from North China and Its Taxonomic Significance. Journal of Paleontology, 2008, 82, 851-855.	0.5	13
52	U–Pb ages and Hf isotopic composition of zircons and whole rock geochemistry of volcanic rocks from the Fangniugou area: Implications for early–middle Paleozoic tectonic evolution in Jilin Province, NE China. Journal of Mineralogical and Petrological Sciences, 2018, 113, 10-23.	0.4	13
53	Bio-Precipitation of Carbonate and Phosphate Minerals Induced by the Bacterium Citrobacter freundii ZW123 in an Anaerobic Environment. Minerals (Basel, Switzerland), 2020, 10, 65.	0.8	13
54	Spatial variation in carbonate carbon isotopes during the Cambrian SPICE event across the eastern North China Platform. Palaeogeography, Palaeoclimatology, Palaeoecology, 2020, 546, 109669.	1.0	12

#	Article	IF	CITATIONS
55	High Mg/Ca Molar Ratios Promote Protodolomite Precipitation Induced by the Extreme Halophilic Bacterium Vibrio harveyi QPL2. Frontiers in Microbiology, 2022, 13, 821968.	1.5	12
56	Extreme halophilic bacteria promote the surface dolomitization of calcite crystals in solutions with various magnesium concentrations. Chemical Geology, 2022, 606, 120998.	1.4	12
57	Research on diagenesis of the sandstone-type uranium deposits in Dongsheng area, Ordos Basin. Science in China Series D: Earth Sciences, 2007, 50, 195-202.	0.9	11
58	Controlling of cements and physical property of sandstone by fault as observed in well Xia503 of Huimin sag, Linnan sub-depression. Science China Earth Sciences, 2013, 56, 1942-1952.	2.3	11
59	A comparison of amorphous calcium carbonate crystallization in aqueous solutions of MgCl2 and MgSO4: implications for paleo-ocean chemistry. Mineralogy and Petrology, 2018, 112, 229-244.	0.4	11
60	Intracellular and Extracellular Biomineralization Induced by <i>Klebsiella pneumoniae</i> LH1 Isolated from Dolomites. Geomicrobiology Journal, 2020, 37, 262-278.	1.0	11
61	Formation Mechanisms of Paleogene Igneous Rock Plays in Huimin Sag, Eastern China. Energy Exploration and Exploitation, 2011, 29, 455-478.	1.1	9
62	Slide origin of breccia lenses in the Cambrian of the North China Platform: new insight into mass transport in an epeiric sea. Geologos, 2012, 18, 223-235.	0.2	9
63	Extracellular, Surface, and Intracellular Biomineralization of <i>Bacillus subtilis</i> Daniel-1 Bacteria. Geomicrobiology Journal, 2021, 38, 698-708.	1.0	9
64	Soft-sediment deformation structures in cores from lacustrine slurry deposits of the Late Triassic Yanchang Fm. (central China). Geologos, 2016, 22, 201-211.	0.2	8
65	Geochemical characteristics of aromatic hydrocarbons in crude oils from the Linnan Subsag, Shandong Province, China. Diqiu Huaxue, 2011, 30, 132-137.	0.5	7
66	Selective Adsorption of Amino Acids in Crystals of Monohydrocalcite Induced by the Facultative Anaerobic Enterobacter ludwigii SYB1. Frontiers in Microbiology, 2021, 12, 696557.	1.5	7
67	Difference in calcium ion precipitation between free and immobilized Halovibrio mesolongii HMY2. Journal of Environmental Sciences, 2022, 122, 184-200.	3.2	7
68	Depositional processes and environmental changes during initial flooding of an epeiric platform: Liguan Formation (Cambrian Series 2), Shandong Province, China. Geosciences Journal, 2018, 22, 903-919.	0.6	6
69	Climatic and tectonic controls of lacustrine hyperpycnite origination in the Late Triassic Ordos Basin, central China: Implications for unconventional petroleum development: Reply. AAPG Bulletin, 2019, 103, 511-514.	0.7	6
70	Calcimicrobes in Cambrian microbialites (Shandong, North China) and comparison with experimentally produced biomineralization precipitates. Carbonates and Evaporites, 2020, 35, 1.	0.4	6
71	Geochemistry and Zircon U-Pb-Hf Isotopes of Metamorphic Rocks from the Kaiyuan and Hulan Tectonic Mélanges, NE China: Implications for the Tectonic Evolution of the Paleo-Asian and Mudanjiang Oceans. Minerals (Basel, Switzerland), 2020, 10, 836.	0.8	6
72	Source–reservoir relationships and hydrocarbon charging history in the central uplift of the south Yellow Sea basin (East Asia): Constrained by machine learning procedure and basin modeling. Marine and Petroleum Geology, 2021, 123, 104731.	1.5	6

ZUOZHEN HAN

#	Article	IF	CITATIONS
73	Mineral compositional controls on the porosity of black shales from the Wufeng and Longmaxi Formations (Southern Sichuan Basin and its surroundings) and insights into shale diagenesis. Energy Exploration and Exploitation, 2018, 36, 665-685.	1.1	5
74	Calcium ion biorecovery from industrial wastewater by Bacillus amyloliquefaciens DMS6. Chemosphere, 2022, 298, 134328.	4.2	5
75	Comparative study on thermal behaviors between micrites and thrombolites using thermogravimetric analysis. Journal of Thermal Analysis and Calorimetry, 2020, 139, 1229-1242.	2.0	4
76	Provenance of the lower Es2 in the Shanghe area of the Huimin sag. Mining Science and Technology, 2010, 20, 453-459.	0.3	3
77	The Late Triassic Molasse Deposits in Central Jilin Province, NE China: Constraints on the Paleo-Asian Ocean Closure. Minerals (Basel, Switzerland), 2021, 11, 223.	0.8	3
78	Distribution of heavy metals in the topsoil of the Jining mining area. Mining Science and Technology, 2010, 20, 395-399.	0.3	2
79	Geochemistry and origin of deep-seated cracked gas on the northern slope of the Dongying Sag, Shandong Province. Diqiu Huaxue, 2011, 30, 353-358.	0.5	2
80	Flash flood as an effective pebble transport mechanism: a case study from the Permian Sulige Gas Field, Ordos Basin, China. Arabian Journal of Geosciences, 2019, 12, 1.	0.6	2
81	Petrogenesis of Silurian ultramafic–mafic plutons in southern Jiangxi: implications for the Wuyi–Yunkai orogen, South China. Geological Magazine, 2021, 158, 1237-1252.	0.9	2
82	Bio-Precipitation of Calcium Ions Induced by Free and Immobilized <i>Virgibacillus dokdonensis</i> WLR1 in Hypersaline Wastewater. Geomicrobiology Journal, 2022, 39, 705-721.	1.0	2
83	Coexistence and inherence of diverse energy resources in the Ordos Basin, China. Diqiu Huaxue, 2006, 25, 386-390.	0.5	1
84	Heavy Metals Distribution Pattern in Coal Gangue. , 2009, , .		1
85	The influence of diagenesis on low-porosity, low-permeability gas reservoirs in the Sulige Gas Field (Ordos Basin, China). , 2022, , 191-215.		1
86	New ages of Early Cretaceous magmatic rocks in the Yanbian area (NE China): implications for the subduction and slab rollback of the Paleo-Pacific Plate beneath eastern China during Early Cretaceous. International Geology Review, 2023, 65, 154-178.	1.1	1
87	Age, provenance and geological significance of (meta)–sedimentary rocks in the Yitong–Gongzhuling area, NE China: Constraints from zircon U–Pb geochronology. Journal of Mineralogical and Petrological Sciences, 2022, 117, n/a.	0.4	1
88	Effects of Chloride, Sulfate and Magnesium Ions on the Biomineralization of Calcium Carbonate Induced by <i>Lysinibacillus xylanilyticus</i> DB1-12. Geomicrobiology Journal, 2022, 39, 852-866.	1.0	1
89	Research of Reservoir Sedimentary Microfacies of Lower Member Es2 in Shanghe Oilfield. , 2009, , .		0
90	Huimin Brush Structural System and Its Influence on Sedimentation and Reservoir Formation. , 2011, , .		0

#	Article	IF	CITATIONS
91	High-Resolution Sequence Stratigraphy in the Lower Member of Es2 in Shanghe Oilfield. , 2011, , .		0
92	Comparison of Geochemical and Mineralogical Characteristics of Palaeogene Oil Shales and Coals from the Huangxian Basin, Shandong Province, East China. Minerals (Basel, Switzerland), 2020, 10, 496.	0.8	0
93	Structural modifications and thermodynamic characteristics of calcite growth during interaction with biomolecular glycine: new insights into biogenesis. Carbonates and Evaporites, 2020, 35, 1.	0.4	0
94	The origin of hyperpycnites in the Middle-Late Triassic Yanchang Fm. (Ordos Basin, China) and their significance for the formation of unconventional hydrocarbons. , 2022, , 337-352.		0
95	Middle-Late Triassic muddy gravity-flow deposits in the Ordos Basin (China). , 2022, , 395-409.		0
96	Facies shifts in the Ordos Basin (China) along the southern and western margins of the North China Plate as a result of plate tectonics. , 2022, , 91-106.		0
97	Biomineralization of Carbonates Induced by Mucilaginibacter gossypii HFF1: Significant Role of Biochemical Parameters. Minerals (Basel, Switzerland), 2022, 12, 614.	0.8	0
98	Amorphous and Crystalline Carbonate Biomineralization in Cyanobacterial Biofilms Induced by <i>Synechocystis</i> sp. PCC6803 Cultured in CaCl ₂ –MgCl ₂ –SrCl ₂ Mediums. Geomicrobiology Journal, 2022, 39, 767-780.	1.0	0
99	Petrogenesis, Magma Source, and Geodynamics of Paleogene Mafic Rocks, Huimin Sag, Jiyang Depression, Eastern China. Geofluids, 2022, 2022, 1-18.	0.3	Ο